

Formation of a through conductive inclusion in a layered sample with sector conductive inclusions in single layers; conductive cluster

R.Ye.Brodskii^{1,2}, *T.V.Kulik*¹

¹Institute for Single Crystals, National Academy of Science of Ukraine,
60 Nauky Ave, 61072 Kharkiv, Ukraine

²V.N.Karazin Kharkiv National University, 4 Svobody Sq.,
61022 Kharkiv, Ukraine

Received July 21, 2022

The results of studying the composition of a through conducting cluster in a layered sample with sector conducting inclusions in round layers are presented. The case of a homogeneous and independent distribution of sector inclusions in each layer is considered. The values of the conductivity of the sample with inclusions and the values of the fraction of the conductive phase in the layer included in the through conductive cluster are obtained for various sets of the system parameters — the number of layers, the number of inclusions in the layer, and the size of the inclusions in the layers.

Keywords: Conductive cluster, layered medium, sector insertions.

Формування наскрізного провідного включення в шаруватому зразку з секторними провідними включеннями в окремих шарах; провідний кластер. *Р.Є.Бродський, Т.В.Кулік.*

Наведено результати дослідження складу наскрізного провідного кластера в шаруватому зразку з секторними провідними включеннями в круглих шарах. Розглянутий випадок однорідного та незалежного розподілу секторних включень у кожному шарі. Отримані значення провідності зразка з включеннями та значення частки провідної фази у шарі, включеної в наскрізний провідний кластер, для різних наборів значень параметрів системи: числа шарів, числа включень у шарі та розміру включень у шарах.

1. Introduction

Layered systems arise in the most diverse areas in nature and are synthesized in technology. If the layers contain inclusions with properties different from the properties of the base material, through volumetric inclusions, for example, conductive ones, may appear in the sample.

Problems about the probability of occurrence of such a conducting cluster and its structure are studied in the theory of percolation. The theory of percolation describes such systems with electrical conductivity, the flow of liquids in media with random

channels, as well as the spread of rumors in social networks. Despite a long history, a significant number of works continue to be published in the field of percolation. The theory finds applications in engineering [1], biology [2], cryology [3].

The behavior of a multilayer physical system near the percolation threshold, the magnetization, was studied in [4]. However, most modern works on percolation in a layered system are devoted to multilayer networks [5–9], where discrete nodes are located in each layer. In present paper, conducting inclusions in layers are considered to be continuous.

Discrete and continuous percolations are the main lines in the development of the theory of percolation. The discrete percolation approach describes the system as a graph or lattice (for example, a square one), i.e. consisting of individual nodes and links. Percolation on lattices is the most developed, however, continues to be studied [10]. In the discrete approach, studies on the spread of infections in networks of human contacts [11–14] and its blocking by immunization [15] are now relevant. In problems of continuous percolation, the flow in a continual non-conducting medium with continual conducting inserts is considered. In classical problems, the "problem of spheres" is considered — round inclusions on a plane and spherical in a three-dimensional case; in modern ones, percolation with inclusions of various other shapes is studied, for example, cylinders with a common preferred direction of axes [16] or arbitrarily oriented [17–18]. The inverse problem was also considered — percolation in a conducting medium, from which cylindrical elements are "excluded" [19].

In this paper, we will consider a discrete-continuous system — continuous in the plane of the layers and discrete in the direction perpendicular to the layers. In [20], a layered sample with inclusions in the form of round "islands" was considered. In this paper, we consider the non-island case of sector inclusions.

In [21], the results of studying the probability of formation of a through conductive inclusion for the problem of sector inclusions are presented. The work presented here is devoted to studying, for the same system, the conductivity of the sample and the composition of the conducting cluster, i.e., the average fraction of the layer included in the conducting cluster.

Among the recent works devoted to the study of the structure of the conducting cluster, one can mention works [22–26], as well as works devoted to the study of the structure of the percolation cluster of the urban system [27], an analogue of the cell membrane, the lipid bilayer [28]. The work [29] is devoted to the study of a percolation cluster on a supercomputer; the work [30] is devoted to the structure of a 4- and 5-dimensional cluster.

In contrast to typical problems of the percolation theory, the paper considers the case when the inclusions have dimensions comparable to the size of the system in the layer plane.

The inclusions-sectors considered in the paper are interesting for two reasons: they are radially symmetric inclusions that can form when the layer grows from the center to the edge, and at the same time they are one-dimensional models. It is useful to consider such one-dimensional models when constructing a theory; and in this case, they also turn out to be equivalent to physically realizable systems.

2. Formulation of the problem

The work is devoted to the study of the composition of a conductive cluster and the conductivity of a layered sample with conductive sector-type inclusions in separate layers.

A sample under consideration consists of N round layers with n identical inclusions-sectors in each layer. Each inclusion has the shape of a sector of size r . The location of the inclusions in layers is random and independent of both the location of other inclusions in the layer and the location of inclusions in other layers.

Let's define ways of measuring the size and position of inclusions.

The inclusion size is understood as follows. The problem under consideration is equivalent to the one-dimensional problem of conducting inclusions-segments in layers-circles. Let us choose the units of measurement of the area of inclusions so that the problems are numerically equivalent, considering the circles to be unit, i.e. with a circumference equal to one. To do this, we will measure the areas of sectors-inclusions in fractions of the area of the entire layer, i.e. we will take the area of the layer as unity. The sectors are naturally set by the angle between the radii bounding the sector; we will measure the angle with a "natural parameter" — i.e. as a part of total turnover. With such methods of measurement, the angular measure of an inclusion numerically coincides with its area and numerically coincides with the length of a segment in an equivalent one-dimensional problem, both for an individual inclusion and for combined inclusions that arise when individual inclusions are superimposed in a layer. We will talk about the angular measure, the area of inclusion or the length of the segment in the equivalent one-dimensional problem, depending on the convenience and clearness visibility in a particular context. This will imply the same value, which is called above the "size" of the inclusion.

The location of the inclusion is understood as follows. The sector inclusion lies between two radii, just as the segment-inclusion in the equivalent one-dimensional problem lies between two points on the circle. The position of the radius will be set by the angle between the given radius and the given reference direction. The angle is laid counterclockwise. The first one, when moving counterclockwise, the radius bounding the given sector, we will call the initial or left radius, the second — the final or right one. The angle from the initial to the final radius, counted counterclockwise, is the same for any inclusion and is equal to the size r . By a random and independent position of an inclusion, we mean a random and independent position of its initial radius.

The paper considers the case of n sectors-inclusions size $r \in (0, 1]$ in all layers.

An example of a layer is shown in Fig. 1.

Fig. 1 shows $n = 5$ inclusions size $r = 0.1$ in the layer. Two inclusions have crossed — the boundaries of each can be traced by measuring the angle observed on non-intersecting inclusions. Further, these two inclusions will be included in the through conducting cluster as one common sector inclusion.

The paper studies the conductivity of the sample and the composition of the conductive cluster — the proportion of the layer substance included in the through conductive cluster, depending on N , n , r .

2. Conductive cluster and conductivity

Considering the conductive regions in each layer, included in the through conductive connection, as cylindrical resistors connected in series, we can find the conductivity of the sample.

Let us take as unity the conductivity of the layer completely filled with the conductive phase. This is convenient, since then, if the through conductive inclusion in this layer occupies an area c , then the conductivity of the layer as a resistor in the chain of resistors will be equal to c .

We can analytically determine the maximum conductivity of the sample. The maximum conductivity of the sample occurs when all layers are completely composed of a conductive phase. In this case, the conductivity of each layer is $c_{max} = 1$ and the conductivity of the entire sample of N layers equal to

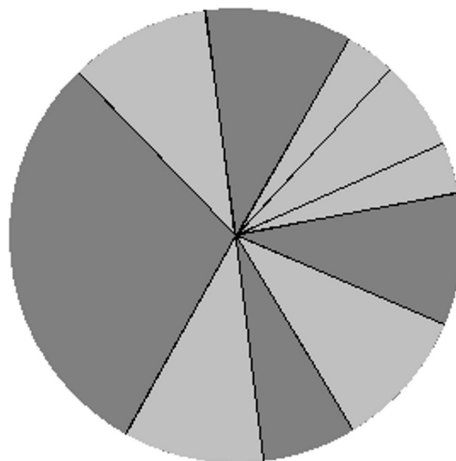


Fig. 1. An example of a layer; dark gray shows a non-conductive part, light gray — conductive inclusions, black — radii limiting individual inclusions.

$$C_{max} = c_{max}/N = \frac{1}{N}. \quad (1)$$

The graphs $C(r)$ Fig.2 below show obtained by modeling averaged values of the electrical conductivity of the sample, depending on the size of a single inclusion r ; for the number of layers $N = 2$ and $N = 5$ and for the number of inclusions $n = 1, 2, 3, 5, 10$ — the graphs from bottom to top. It can be seen that the values of the average conductivity tend to a maximum equal to $C_{max} = 1/N - 0.5$ for $N = 2$ and $1/5$ for $N = 5$.

For larger N , the graphs are closer to the horizontal axis and their analysis becomes difficult. You need to use rescaled graphs — with values multiplied by N , then the maximum for all graphs will be equal to one. However, the conductivity values C multiplied by N have their own independent meaning. The values $C \cdot N$ are equal to the conductivity values for one layer, averaged both over the experiments and over the layers in the sample, $c = C \cdot N$.

These values coincide with the averaged **part of the layer included in the through inclusion**. These values do not coincide with the degree of filling, i.e. the proportion of the conductive part of the layer to the area of the layer, since not all of the conductive phase in the layer can be included in the through conductive inclusion. Some part of the conductive phase in the layer may not have contact with conductive regions in neighboring layers or enter into conductive clusters that do not reach the boundary layers, but lie inside the sample or reach only

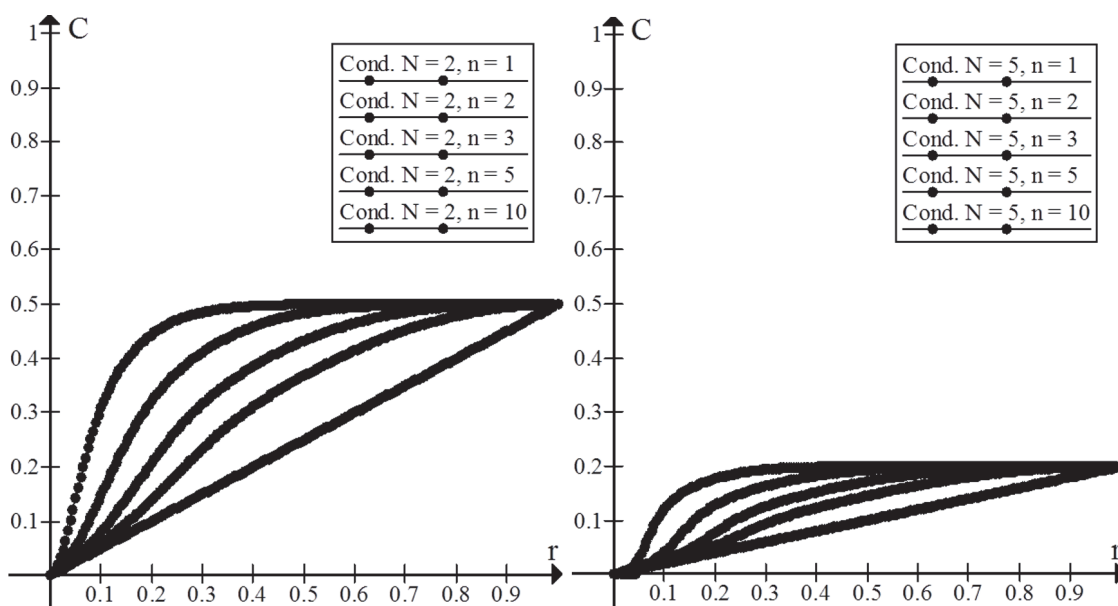


Fig. 2. Average conductivity for the samples with the number of layers $N = 2$ on the left, and $N = 5$ on the right; in each figure, the graphs correspond to the number of inclusions in the layer $n = 1, 2, 3, 5, 10$, from bottom to top.

one of the boundary layers — the lower or upper.

This value — the average fraction of the layer, which is included in the through conductive inclusion, is of great importance from the point of view of describing the through conductive inclusion, the conductivity cluster. Further in this section, we will discuss exactly this quantity — the conductivity per layer. The conductivity of the sample as a whole will have the same behavior, only with a smaller value by a factor N .

Fig. 3 shows the graphs: $c(r)$ versus the size of a single conductive inclusion — on the left, and $c(s)$ versus the filling — on the right; for $N = 2$, and $N = 10$ top and bottom respectively. The graphs are shown for $n = 1, 2, 3, 5, 10$ — from bottom to top for graphs vs r , and marked with different labels for graphs vs s .

The graphs of $c(r)$ and $c(s)$ for $n = 1$ coincide, since the filling of the layer at $n = 1$ is equal to the size of a single inclusion. For a given value n , the graphs of the average conductivity per layer for both N are a straight line with a unit slope. This is due to the appearance of a conducting inclusion in the sample; since the conductivity values are determined only for such cases, then, with a single inclusion in the layer, it is guaranteed to be completely included in this through conductive inclusion, so that $c = s = r$.

For $n > 1$ larger values of filling, the $c(s)$ graphs are close to a straight line for $n = 1$, since at high filling values, all conductive

regions in the layer merge into one and the situation is the same as in the case of a single inclusion: if a through inclusion appears at all, then the conductive phase in each layer enters it entirely, $c = s$.

Note, that the graphs $c(r)$ for consecutive increasing n are arranged from bottom to top, while the graphs $c(s)$, as can be clearly seen in the figure for $N = 10$, are arranged from top to bottom despite the fact that the set of ordinate values c the same, and the filling values s versus r monotonically increase. This is due to different rates of increase of s with r for different n . As a result, at large n , the area of small r expands significantly when passing to s , while the area of large r shrinks; so, for example, for $N = 10$ and $n = 10$, about a half of the points of the $c(r)$ graph, the points with ordinates close to one, are projected to one point with $s = 1$.

The graphs $c(s)$ at $n > 1$ pass under the line of $c = s$, since at $n > 1$, part of the conductive phase in the layer may not be included in the through connection, therefore, the fraction of the phase included in the through connection, c , turns out to be less than filling (the ordinate of the point is less than the abscissa). At the same time, the average fraction of the layer included in the through inclusion at $n > 1$ is larger than the size of a single inclusion, even if the inclusions overlap in the layer, so that the graphs $c(r)$ (left) pass over the line of $c = r$.

Also for large N , there is a jump in the initial region of the graphs. This is not re-

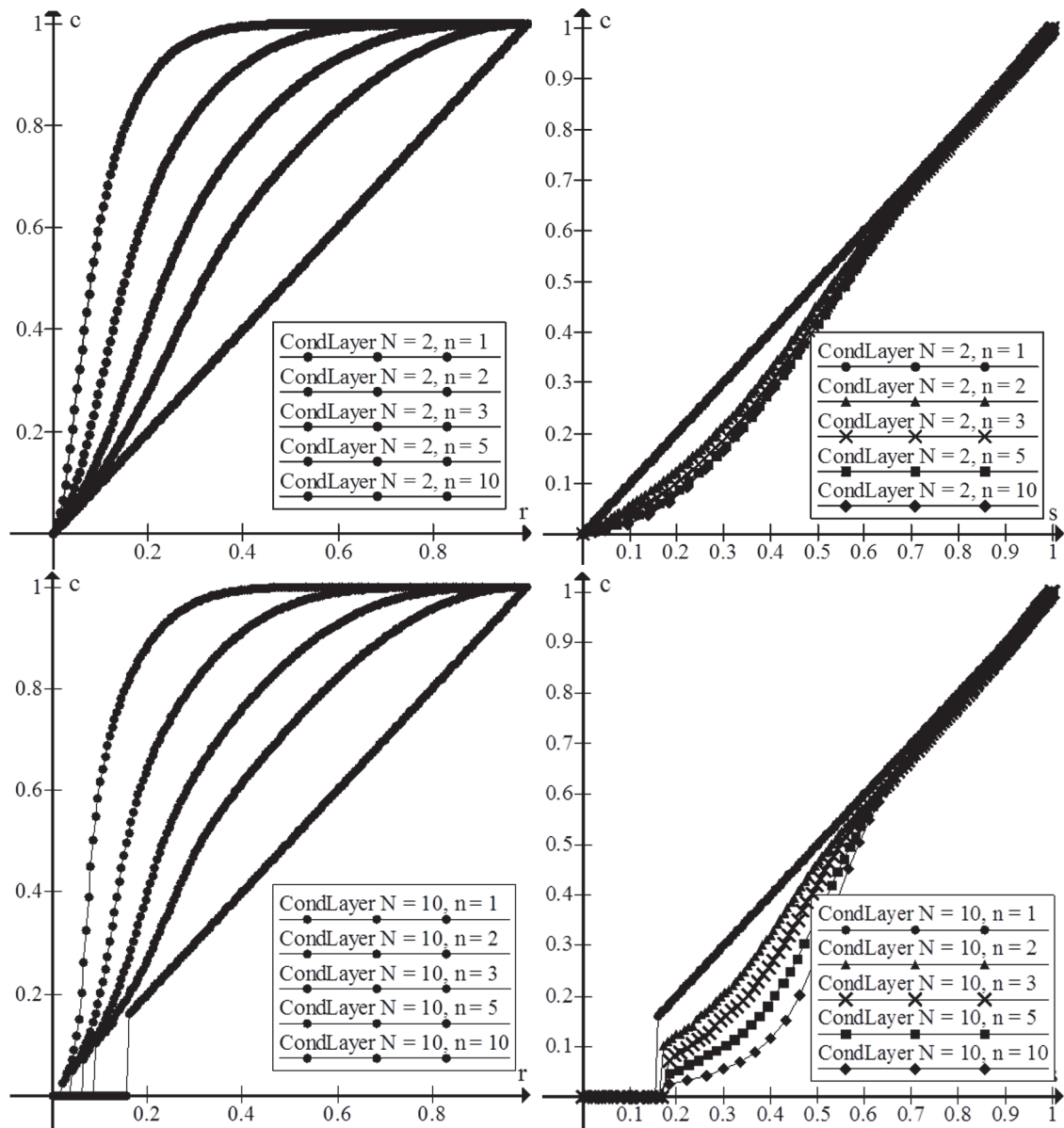


Fig. 3. Average conductivity per layer $c(r)$ as a function of the size of the individual inclusion — on the left, and $c(s)$ as a filling function — on the right, for the number of layers $N = 2$ top and $N = 10$ bottom; graphs on each figure correspond to the number of inclusions in the layer $n = 1, 2, 3, 5, 10$, for $c(s)$, they marked with different labels.

lated to the properties of the system, but is due to the fact that at large N for given small r or s in all experiments (10,000 of them were carried out for each r), not a single sample with a through conductive inclusion appeared. It would be possible to advance into this area by increasing the number of experiments, however, since general course of graphs with N does not change, the appearance of new effects in this area is not expected, and an increase in the number of experiments would increase the simulation time. However, we will return to this effect later.

As you can see, the graphs as a function of r , change less with changing N , than the graphs as a function of s ; therefore, to save space, we present the graphs only as a function of s for the remaining $N = 3, 5, 50, 100$. On Fig. 4, the graphs are shown for the listed N ascending from left to right and top to bottom.

Comparing graphs for $N = 2, 3, 5$ you can see that the difference between the graphs for different n increases with the number of layers N ; for large $N = 50, 100$, the "zero region" occupies a significant part of the graphs, but from the rest is clear, at least

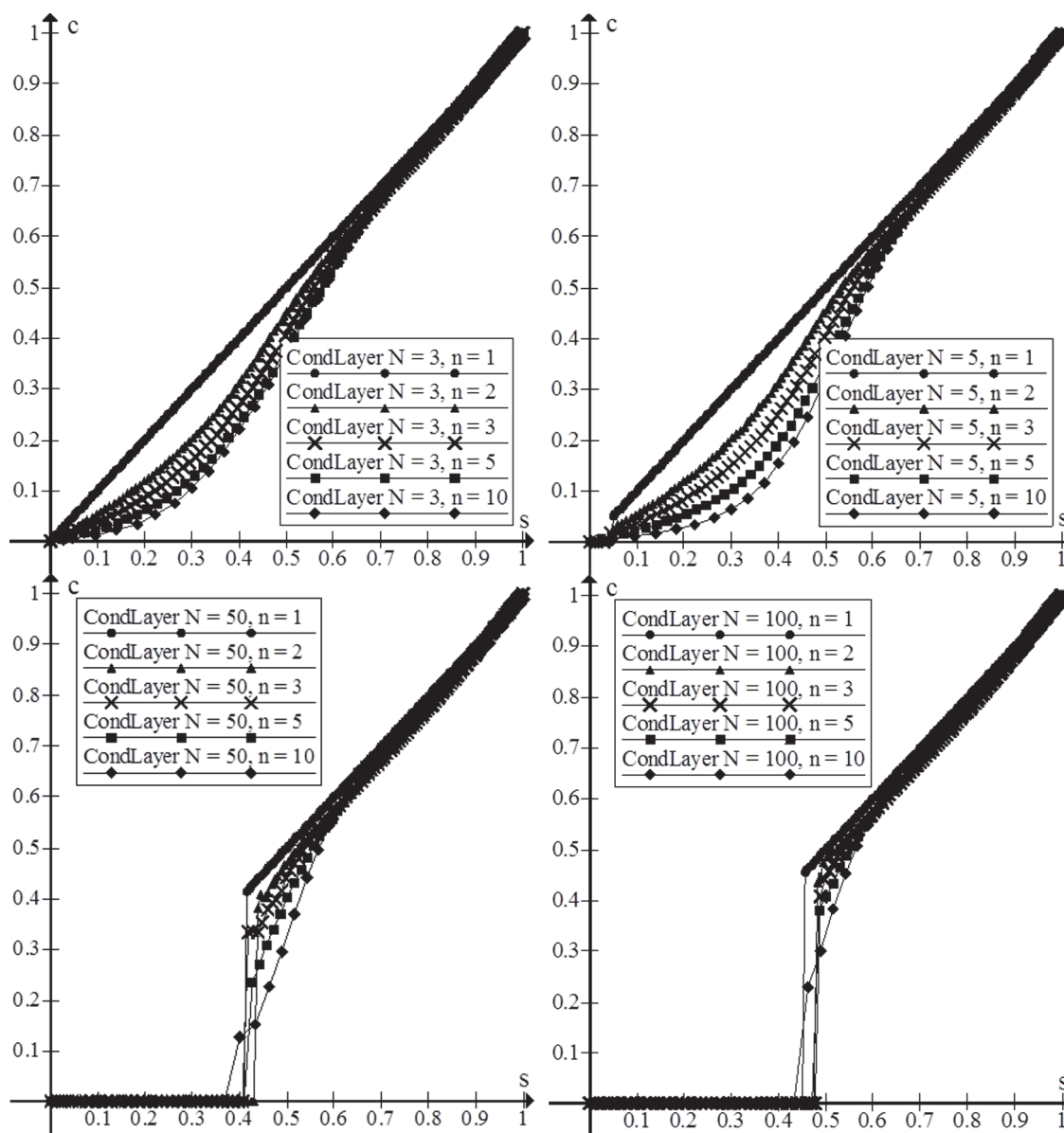


Fig. 4. Average conductivity per layer $c(s)$ as a fill function, for the number of layers $N = 3, 5, 50, 100$ from left to right and from top to bottom, graphs in each fig. correspond to the number of inclusions in the layer $n = 1, 2, 3, 5, 10$, marked with different labels.

for $N = 50$, that this trend persists even with such N , and also that the order of the graphs from top to bottom in ascending order of n is preserved.

This order is due to the fact that with an increase in n , the fragmentation of the conductive phase in the layer increases with the same filling, so that an increasing part of the conductive phase can fall out of the through conductive inclusion. The order of the graphs $c(r)$ from bottom to top is due to the fact that with an increase in n , the growth rate of the part of the conducting phase in the layer with r also increases.

As mentioned above, it is also seen that the boundary of the "zero region" shifts to the right with increasing N . We will consider this issue in more detail later, but we immediately note that for all N up to very large, the boundary of the zero region on the graphs $c(s)$ for given N is almost the same for all n . This property is just for graphs from filling; on the graphs $c(r)$, the boundary of the zero region for different n falls on different r . This is already noticeable for $N = 10$ on the graphs above, and even more noticeable at large N , for example, for $N = 100$, the graphs $c(r)$ have the following form (Fig. 5).

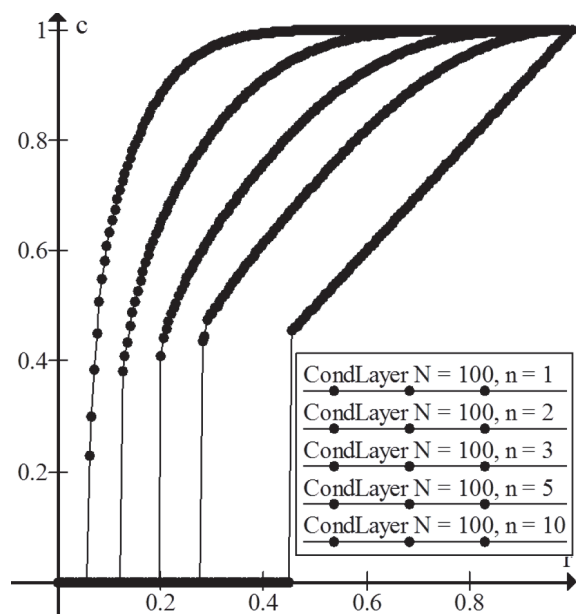


Fig. 5. Zero region on graphs for different of average conductivity per layer $c(r)$ as a function of the individual inclusion size for the number of layers $N = 100$; the graphs correspond to the number of inclusions in the layer $n = 1, 2, 3, 5, 10$, from bottom to top.

It is more convenient to analyze in more detail the change in the type of graphs with N on graphs for different N at one n in Fig. 6. As mentioned above, the graph for $n = 1$ does not change with N and has the form of a straight line with a unit slope. Consider graphs various N at $n = 2, 3, 5, 10$. The following figure 6 shows a series of graphs for the listed n from left to right and from top to bottom.

It can be seen that at small n , i.e. small fragmentation of the conductive phase in the layer, the graphs for different N differ little from each other. At $n = 5, 10$ the differences are noticeable.

Outside the zero region, the graphs with $n = 5$ are arranged from top to bottom in ascending order N : the more N , the greater the deflection of the graph, as we noted above. At $n = 10$, the graphs for $N = 2, 3, 5, 10$ are arranged from top to bottom, but the graphs for $N = 50, 100$, outside their zero region, overtake at least the graph for $N = 10$. Note that the overtaking by graphs for very large values of the parameter of graphs arrange for lower values of the same parameter arrange in a certain order, we have already noted in [21] earlier for the graphs $P(s)$. Obviously, such an overtaking means that at large values of the parameter, other new mechanisms begin to

influence the shape of the graph, which do not appear at small values of the parameter.

It is possible to raise the question of what part of the conductive phase in the layer is included in the conductive inclusion ($c(r)$ — part of the entire layer), i.e. to find c/s . Below, Fig.7, are graphs of this value against r ; are given to save space, the graphs are shown only for $N = 2, 5, 10, 100$.

For the reasons described above, the graph at $n = 1$ for all N looks like $c/s = 1$.

Other graphs behave as follows. In the area of small r , the graphs are arranged from top to bottom in ascending order of n , from $n = 2$ to $n = 10$, but after the transition region, the graphs are swapped and arranged in ascending order of n upwards. Obviously, this is due to the fact that at small r , the dominant role is played by the higher one at large n fragmentation, but with increasing r , the fragmentation value decreases, and the total size of the conducting phase in the layer begins to dominate, increasing with increasing n .

Graphs at $n > 1$ differ most from unity at small r and tend to unity with increasing r (the conductive phase in the layer tends to merge into one).

Note that when $r > 0.5$, inclusions in the layers necessarily merge into a single whole, small (~ 0.01) differences from unity in the position of the graph points at $r > 0.5$ are explained only by the fact that the values of c/s are obtained as a result of quite a few computational operations — each with limited accuracy.

You can also build graphs c/s against s ; however, the presence of a calculated (rather than a control) parameter in determining the position of points both along the horizontal and vertical axes makes the analysis of such graphs unnecessarily confusing.

The zero regions on the graphs, as mentioned above, are due to the fact that, with the appropriate values of the parameters, in none of the experiments out of 10,000, a through conductive inclusion was formed. This means that the boundary of the zero region approximately shows the value of the parameter of filling, if we are talking about the boundary on the graphs from filling s , at which the probability of forming a through conductive inclusion is equal to $1/10000$. Determination of the corresponding point directly from the probability graph $P(s)$ is difficult.

The zero region is also on the graphs $c(r)$, however, at different r , and on the

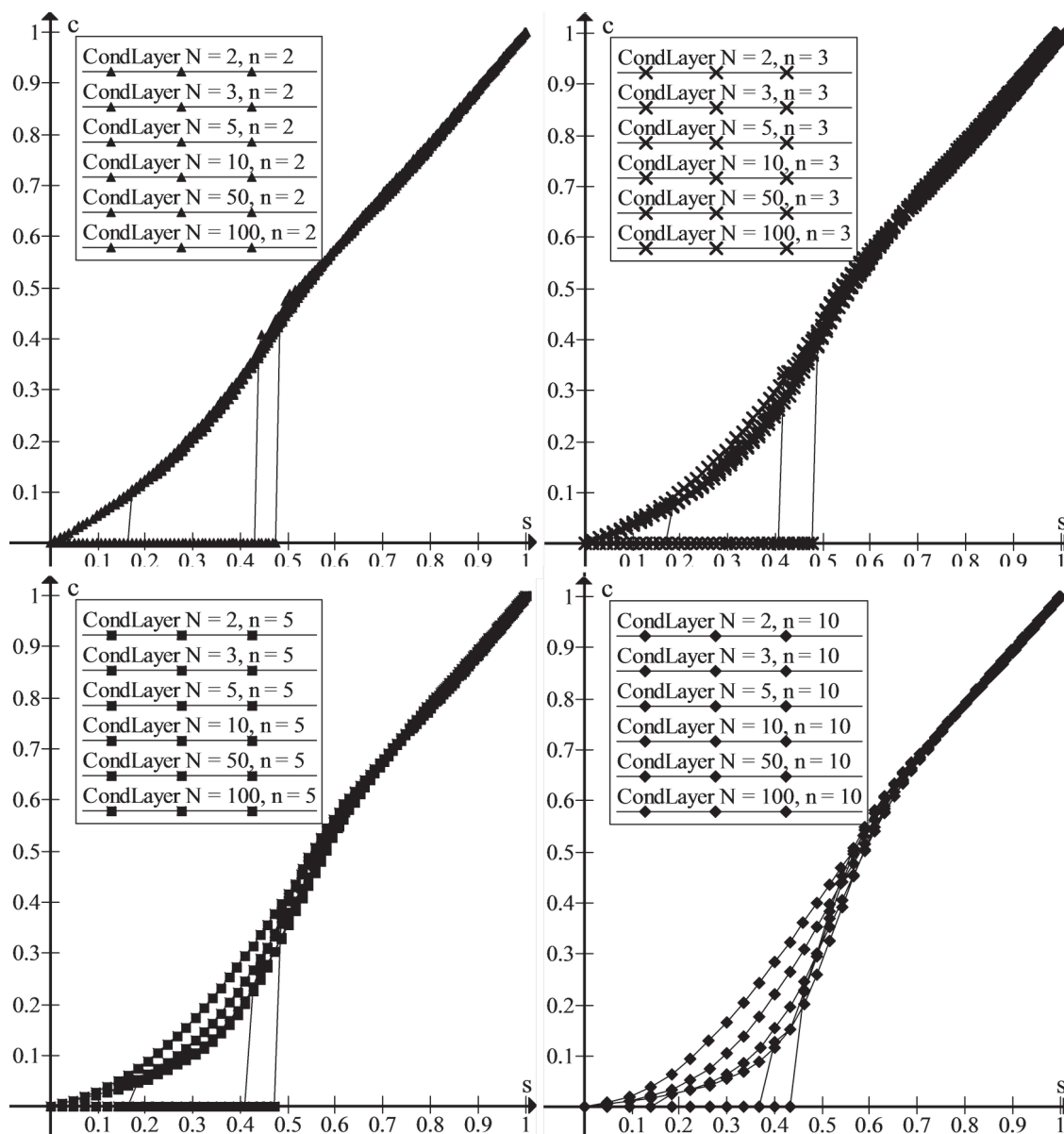


Fig. 6. Average conductivity per layer $c(s)$ as a filling function for the number of inclusions in the layer $n = 2, 3, 5, 10$ from left to right and from top to bottom; graphs in each figure correspond to the number of layers $N = 2, 3, 5, 10, 50, 100$.

graphs from filling it is located in approximately the same place for all n ; i.e. it can be assumed that for a given number of layers N the boundary of the zero region is determined only by the filling value s , but not r and n separately, and you can raise the question of the position s_0 of boundaries of the zero region for a given number of experiments as a function of N . On the next figure 8, the values $s_0(N)$ of the boundary of the zero regions found from the simulation are shown for various N corresponding to the number of experiments 10000.

The smooth curve shows the analytically found function $s_0(N)$ at 10,000 experiments, proposed from the following considerations.

When only one inclusion is present in each layer, i.e. $n = 1$, or when all inclusions merge into one, the probability of forming a through conductive inclusion decreases exponentially with the number of layers, since to form a through inclusion, it is necessary that conducting inclusions have contact in all adjacent layers; and if the filling of a layer is the same in all layers, then the probability P_N of the formation of a conduc-

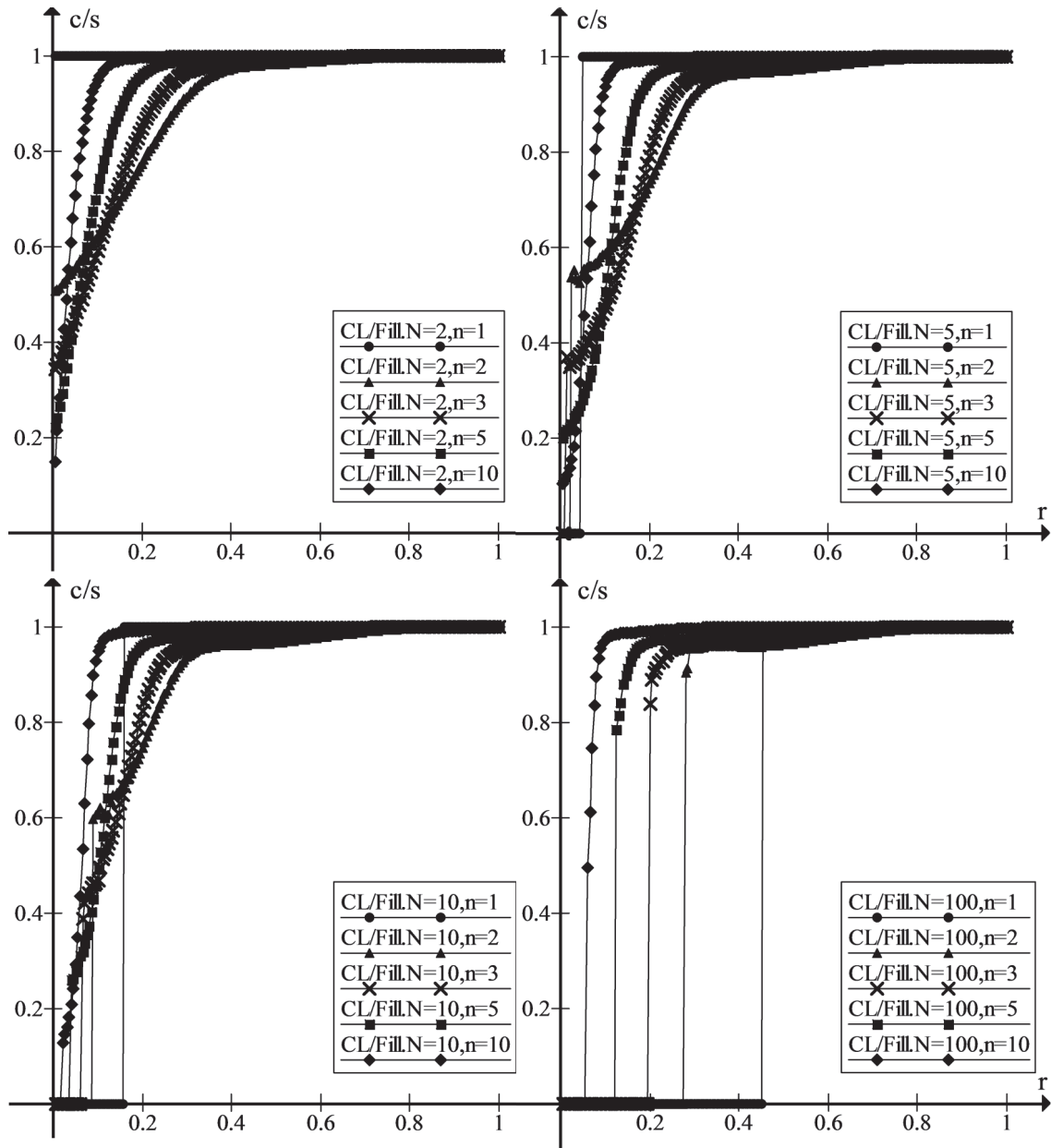


Fig. 7. Fraction of the conductive phase of the layer included in the through conductive cluster, c/s as a function of individual inclusion size for the number of layers $N = 2, 5, 10, 100$ from left to right and from top to bottom; graphs in each figure corresponding to the number of inclusions in the layer $n = 1, 2, 3, 5, 10$ are marked with different labels.

tive inclusion in N layers with a given filling is equal to $P_N = (P_2)^{N-1}$, where P_2 is the probability of the formation of a conductive inclusion in a sample of two layers with the same filling or, which is the same, the probability of contact of the conductive phases in a pair of adjacent layers. As shown in [21] in the section studying of the case of $n = 1$, the probability $P_N(s)$ depends on filling s at $s < 0.5$ as

$$P_N(s) = (2s)^{N-1},$$

at $s > 0.5$, the probability is equal to one. Hence, in the case of such an exponential dependence on N , the zero region boundary, s_0 , at which the probability reaches the value $1/10000$, would depend on N as

$$s_{0,P=1/10000}(N) = \frac{1}{2} \left(\frac{1}{10000} \right)^{\frac{1}{N-1}}.$$

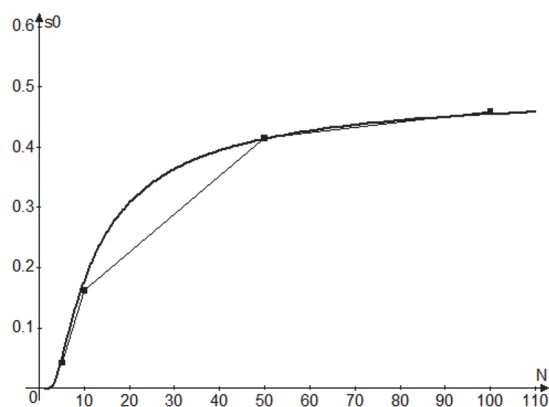


Fig. 8. Zero region boundary on graphs $c(s)$ for various N .

When there can be more than one inclusion in each layer, contact between inclusions in each pair of adjacent layers is not enough, since in some layer, one part of the conducting phase can have contact with the previous one, and another part that does not contact the first one in the layer is in contact with the next layer; thus, the decrease in the probability of forming a through inclusion with the number of layers is superexponential.

However, it is the function obtained above that is plotted on the graph $s_0(N)$, and as you can see, it matches very well with the points obtained in the simulation. Differences may be due to inaccuracy in the definition s_0 from the graphs associated with the final step of plotting, and taking into account the fact that for different n with the same N , the values s_0 on the graphs are slightly different, the value of s_0 is determined approximately. The values s_0 were determined approximately in the middle of a rather narrow range of the zero region boundaries for different n .

Such a coincidence suggests that in the region of very low probabilities, the dependence $P_N(s)$ from N at n , other than unity, is approximately exponential — the same as for $n = 1$; note, however, that in general case, the graphs for different n noticeably differ, so that the studied quantities are different for different n .

Conclusions

1. The values $C(r)$ of conductivity of the sample were obtained as a circuit of a series of resistors; each resistor is a conductive part of one layer, which is included in a through conductive cluster. It is shown that

the values $C(r)$ at $r \rightarrow 1$, tend to the theoretical maximum possible for a sample from N layers, $C_{max}(N) = 1/N$ (Fig. 2).

2. The values $c(r)$ of average fraction of the layer, which is included in the through conductive cluster, were obtained as a function of size r of a single inclusion, (Fig. 3). The functions $c(r)$ monotonically increase from 0 to 1. The values $c(r)$ at given r for different number of inclusions are monotonically increasing with n .

3. The values $c(s)$ of a fraction of the layer which is included in the through conductive cluster were obtained as a function of the average layer filling s , (Figs. 3, 4, 6).

a. At $n = 1$, the values $c(s)$ match with $c(s) = s$, since with a single inclusion in a layer, the inclusion in each layer is guaranteed to be completely included in the through inclusion.

b. At $n > 1$, the functions $c(s)$ tend to a straight line, $c(s) = s$ at $s \rightarrow 1$. The reason is that with increasing filling, the fragmentation of the conductive phase in the layer decreases until the conductive regions merge into one, then the entire conductive phase enters the conductive cluster, $c(s) = s$.

4. In the case $n > 1$ for $s < 1$, the values $c(s) < s$, since the conducting cluster includes no more part of the layer than the part filled with the conducting phase.

a. The difference of $c(s)$ from s increases with n , since with increasing n , the fragmentation of the conducting phase increases.

b. The difference of $c(s)$ from s for various N is insignificant for small n . At large n , the difference increases with N , i.e. $c(s)$ decreases with N for $N = 2, 3, 5, 10$, but at very large $N = 50, 100$, the functions $c(s)$ starting from some s overtake $c(s)$ for smaller N .

5. Dependencies c/s — part of the conductive phase in the layer, which is included in the through cluster, — were obtained as a function of r , Fig. 7.

a. For $n = 1$, the dependence looks like $c/s = 1$, since $c(s) = s$ for the reasons indicated in paragraph 3a.

b. For $n > 1$, at small r , the values of c/s decrease with n , but at some r , the graphs for large n overtake the graphs for smaller ones (at different r for different couples of n); and after region of overtaking, the graphs are arranged from bottom to top in ascending order of n . This is due to the fact that at small sizes r of individual inclusions, the fragmentation of the conducting phase in the layer has a great influence,

which increases with an increase in n , but for large r , the inclusions merge with the greater probability, the more n .

6. Values s_0 of fillings corresponding to the probability of formation of a conductive inclusion $P = 1/E$ were obtained, where E is number of experiments, Fig. 8.

a. For $n = 1$, the values s_0 as a function of N were obtained analytically, $s_0(N) = 1/2(1/E)^{1/N-1}$, $E = 10000$ is number of experiments used in the simulation.

b. It is shown that the values s_0 do not depend on n .

References

1. C.-W.Nan, Y.Shen, Jing Ma, IAnnu. Rev. Mater. Res., **40**, 131 (2010).
2. E.Kroener, M.Ali Ahmed, A.Carminati, *Phys. Rev. E*, **91**, 042706 (2015).
3. S.Marchenko, J.J.van Pelt Ward, Claremar Bjorn et al., *Frontiers in Earth Science*, **5**, 16 (2017).
4. H.G.Silva, A.M.Pereira, J.M.Teixeira et al., *Phys. Rev. B*, **82**, 144432 (2013).
5. M.De Domenico, C.Granell, M.A.Porter, A.Arenas, *Nat. Phys.*, **12**, 901 (2016).
6. Yan-Yun Cao, Run-Ran Liu, Chun-Xiao Jia, Bing-Hong Wang, *Communications in Non-linear Science and Numerical Simulation*, **92**, 105492 (2021).
7. R.R.Liu, D.A.Eisenberg, T.P.Seager et al., *Sci. Rep.*, **8**, 2111 (2018).
8. Wang Xiao Juan, Guo Shi Ze, Jin Lei, Wang Zhen, *Physica A: Statistical Mechanics and its Applications*, **471**, 233 (2017).
9. Andrea Santoro, Vincenzo Nicosia, *Phys. Rev. Research*, **2**, 033122 (2020).
10. R.K.Akhunzhanov, A.V.Eserkepov, Y.Yu.Tarasevich, *J. Phys.A: Math.Theor.*, **55**, 204004 (2022).
11. R.M.Ziff, *Physica A: Statistical Mechanics and its Applications*, **568**, 125723 (2021).
12. H.E.Roman, F.Croccolo, *Mathematics*, **9**, 3054 (2021).
13. M.Dickison, S.Havlin, H.E.Stanley, *Phys. Rev. E*, **85**, 066109 (2012).
14. S.-W.Son, G.Bizhani, C.Christensen et al., *EPL*, **97**, 16006 (2012).
15. P.Clusella, P.Grassberger, F.J.Perez-Reche, A.Politi, *Phys. Rev. Lett.*, **117**, 208301 (2016).
16. D.Jeuilin, M.Moreaud, *Image Analysis and Stereology*, **26**, 121 (2007).
17. A.Golovnev, M.E.Suss, *J. Chem. Phys.*, **149**, 144904 (2018).
18. D.Sangare, P.M.Adler, *Phys. Rev. E Stat. Nonlin. Soft Matter Phys.*, **79**, 052101 (2009).
19. J.Tykesson, D.Windisch, *Probability Theory and Related Fields*, **154**, 165 (2012).
20. R.Ye.Brodskii, *Funct. Mater.*, **27**, 159 (2019).
21. R.Ye.Brodskii, *Funct. Mater.*, **29**, 419, 2022
22. Y.S.Cho, S.Hwang, H.J.Herrmann, B.Kahng, *Science*, **339**, 1185 (2013).
23. S.Armstrong, P.Dario, *Comm. Pure Appl. Math.*, **71**, 1717 (2018).
24. M.Gorny, E.Maurel-Segala, A.Singh, *Ann. Inst.H. Poincare Probab. Statist.*, **54**, 2238 (2018).
25. Pengfei Tang, *Ann. Probab.*, **47**, 4115 (2019).
26. P.Trapman, *Ann. Probab.*, **38**, 1608 (2010).
27. T.Fluschnik, S.Kriewald, A.Garcia Cantu Ros et al., *ISPRS International Journal of Geo-Information*, **5**, 110 (2016).
28. N.Nisoh, V.Jarerattanachat, M.Karttunen, J.Wong-ekkabut, *Biochimica et Biophysica Acta (BBA) — Biomembranes*, **1862**, 183328 (2020).
29. S.Y.Lapshina, *Lobachevskii J. Math.*, **40**, 341 (2019).
30. X.J.Tan, Y.J.Deng, J.L.Jacobsen, *Front. Phys.*, **15**, 41501 (2020).